
J. Kenneth Salisbury John J. Craig

Department of Computer Science
Stanford University
Stanford, California 94305

Articulated Hands: Force Control and Kinematic Issues

Abstract

Kinematic and control issues are discussed in the context of an articulated, multifinger mechanical hand. Hand designs with particular mobility properties are illustrated, and a definition of accuracy points within manipulator workspace is given. Optimization of the physical dimensions of the Stanford-JPL hand is described. Several architectures for position and force control of this multiloop mechanism are described, including a way of dealing with the internal forces inherent in such systems. Preliminary results are shown for the joint torque subsystem used in the hand controller.

1. Introduction

Research activity in manipulation has been generally focused on arms with six degrees of freedom and end effectors capable of only simple grasping. Two problems with current systems are that (1) they are unable to adapt to a wide range of object shapes and (2) they are unable to make small displacements at the hand without moving the entire arm. This limits the response and fidelity of force control to that of the whole arm even for very small motions. Ironically, the most critical and necessarily accurate motions in an assembly task are of small magnitude.

J. Kenneth Salisbury is currently a graduate student in the Department of Mechanical Engineering at Stanford University and is a student member of the IEEE and the ASME. John J. Craig is currently a graduate student in the Department of Electrical Engineering at Stanford University and is a student member of the IEEE.

This research was supported by National Science Foundation research grant DAR78-15914 and Cal-Tech President's Fund Grant CIT PF186.

The International Journal of Robotics Research
Vol. 1, No. 1, Spring 1982,
0278-3649/82/010004-14 \$05.00/0
© 1982 Massachusetts Institute of Technology

Once a manipulator has placed objects to be assembled in contact with each other, the subsequent, partly constrained motions necessary to complete the assembly are often less than 1 cm, with angular excursions of less than 20°. Thus, joints that are designed to move through a working volume with a radius of 0.5 m or more are used to make small, critical movements.

One solution to this problem has been to use small, motion-producing devices between the end effector and the arm. The remote center compliance (RCC) device from Draper Laboratories (Drake 1977) is an example of a passive approach. The three-axis, force-controlled assembler developed by Hill at SRI is an example of an active, small-motion device. In both these solutions, the end effectors are suited only for static grasping, not for both the moving and grasping functions. This approach limits manipulative ability in two ways. First, the lack of a stable adaptive grasp necessitates tool changes or limits the class of manipulatable objects. Second, by placing the mass of the gripper and its actuator after the small motion device, a lower bandwidth for a given input power is imposed on the motion.

Numerous designs for multifinger hands suited for grasping only have been developed (Childress 1972; Skinner 1975; Crossley and Umholtz 1977; Rovetta 1977). These designs have almost exclusively been aimed at approximating a subset of human grasping patterns observed to be useful in human function. A three-finger design with a total of 11 degrees of freedom has been described by Okada (1977) that uses a heuristic combination of position and force-controlled fingers to grasp objects and impart some limited motion. It does not, however, address the problem of general motion of grasped objects. Though the anthropomorphic model may be useful, we should not limit the analysis to the duplication of human motion.

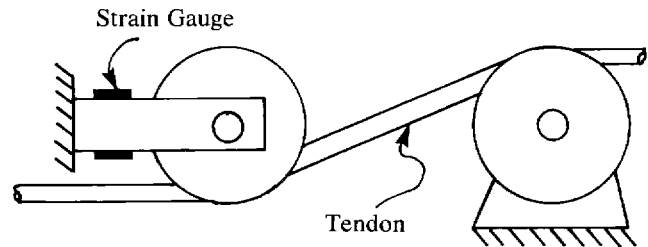
The process of grasping can be treated analytically with well-developed kinematic methods. We con-

Fig. 1. Cable-tension sensor.

sider an object to be securely grasped when it is immobilized by contact with its surroundings (i.e., fingers). If only frictionless point contact is made with the body, seven contacts are generally needed (Lakshminarayana 1978). This would present a formidable design problem. Furthermore, designs using only frictionless contacts could not apply moments about the axis of symmetry of common objects such as cylinders and spheres. In the analysis that follows, we will consider friction at contact points and identify several possibly acceptable designs. Of these, we will focus on a three-finger hand with 9 degrees of freedom. With this design, general forces or small motions can be imposed on securely grasped objects held in tip prehension. This hand is also capable of a variety of other prehensile patterns for securing objects, including the cylindrical, spherical, pinch, and lateral pinch grasps identified by Schlesinger (1919).

In a collaborative effort between Stanford University and Jet Propulsion Laboratory (JPL), the design and fabrication of such a hand, the Stanford-JPL hand, has been undertaken. Intended for retrofitting of existing manipulators, Stanford-JPL hand system has motors mounted on the forearm and flexible conduit that carry Teflon-coated tension cables around the wrist joints. By placing the hand actuators on the forearm of the manipulator, we reduce the gravity-loading and inertial effects of the hand actuators on the rest of the system. The hand size is greatly reduced, and durability is increased by not having the actuators inside the fingers. To ensure accurate sensing and control of forces at the fingers, a cable-tension-sensing mechanism is placed on each cable where it enters a finger. The cantilever beam shown in Fig. 1 supports an idler pulley around which the cable is deflected. By measuring the strain at the base of the beam it is possible to infer the tension in the cable. This allows us to close a tension-control loop around the major sources of friction in the system (motor brushes, gears, and conduit). The sensor is in the same frame of reference as the actuator so that no coordinate transformation is necessary for tension control.

As in some other designs (Morecki 1980), tendon tensions are combined at the joints so as to permit use of only four actuators for each three-degrees-of-



freedom finger and no pre-tensioning of the cables. A more detailed description of the mechanism design has been presented elsewhere (Salisbury and Ruoff 1981). During grasping, the fingers and grasped object form one or more closed-loop kinematic chains. This necessitates the control architecture described later for dealing effectively with internal forces and physical constraints imposed on the cooperative motion of several fingers.

2. Mobility Analysis

To determine the instantaneous mobility of rigid objects grasped in various ways, we must model the constraints on object motion imposed by contacts with fingers in the gripping system. The motion of an unconstrained body is partially restricted when it is brought into contact with another object such as a finger link. Additional contacts further reduce the object's availability of motion until ultimately it is completely restrained from motion. The type and location of these contacts determine the extent to which motion is restricted. The type of contact can be classified by the degrees of freedom of relative motion it permits between two contacting bodies (in lieu of any other constraint). Degrees of freedom are listed in Table 1. The term *soft finger* (see Table 1) is used to denote a contact area with friction that is great enough to resist moments about the contact normal. In this case, rolling without slip across the contact area is possible, but translation at the contact area is precluded by frictional forces or structural restraint.

The classic kinematic approach is to consider contact without friction. In this approach, motion is lim-

Fig. 2. Ball-and-socket mechanism in which $M = 6$ and $C = 5$.

Table 1. Contact Types

Degrees of Freedom	Examples
0	Glue, planar contact with friction
1	Line contact with friction, revolute joint
2	Soft finger
3	Point contact with friction, planar contact without friction
4	Line contact without friction
5	Point contact without friction
6	No contact

ited only by structural restraint. In reality, restraint due to frictional forces is often present and necessary in common manipulative operations. Without friction, most manipulator end effectors would be unable to grasp common objects. We assume that internal or external forces in grasping will be appropriate to maintain force closure (Reuleaux 1963) and will be of sufficient magnitude so that constraints resulting from friction will be maintained (remain active).

The mobility, M , of a kinematic system is defined as the number of independent parameters necessary to specify completely the position of every body in the system at the instant of concern. To compute the mobility, we use Grübler's formula (Hunt 1978) in a modified form.

$$M \geq \sum f_i + \sum g_i - 6L \quad (1)$$

$$M' \geq \sum g_i - 6L \quad (2)$$

where

M = mobility of system with finger joints free to move;

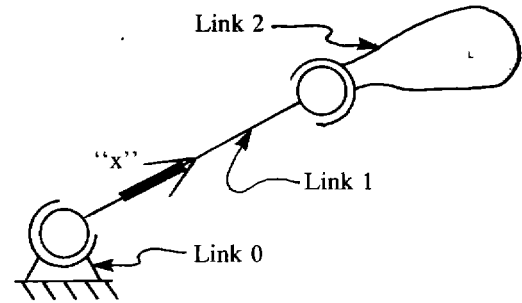
M' = mobility of system with finger joints locked;

f_i = degrees of freedom in i th joint (considered to be 1 here);

g_i = degrees of freedom of motion at i th contact point (1-5);

L = number of independent loops in system.

The inequality in these relations results from the fact



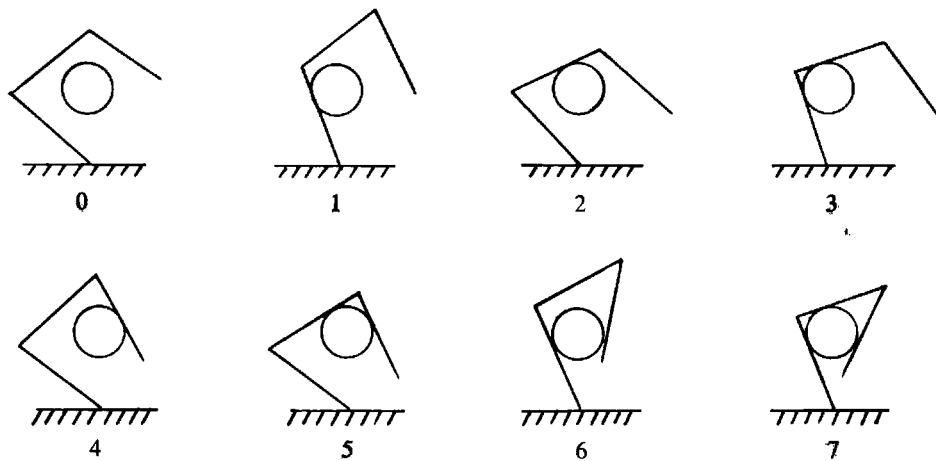
that constraints on the motion of a body in the system may not be independent. In this case, strict equality would indicate fewer degrees of freedom of motion than are actually possible. We are concerned with the relative motion (or lack of it) between a grasped object and the palm of the hand. The connectivity, C , between two particular bodies in a kinematic system is defined as the number of independent parameters necessary to specify completely the relative positions of the two bodies at the instant of concern. We will use C to denote the connectivity between the palm and the grasped object.

To illustrate the difference between mobility and connectivity, consider the mechanism in Fig. 2. Two ball-and-socket joints (three degrees of freedom each) are connected by a rigid link. $M = 6$ because six parameters will locate completely all the parts of the mechanism. The connectivity between link 0 and link 2 is 5, however, because the parameter specifying the rotation of link 1 about its "x" axis is not needed to locate link 2 relative to link 0.

Connectivity may be derived from mobility by considering the two bodies in question as fixed and determining the mobility of each subchain connecting them. In the case of a hand, this will mean fixing the object relative to the palm and determining the mobility of each finger subchain. Subchain mobilities greater than 0 are then subtracted from overall system mobility to yield the connectivity. This procedure, worked out during conversations with Prof. B. Roth at Stanford University, has the effect of eliminating from consideration motions in the mechanism that can be made without affecting the motion of the grasped object.

Requirements for the Stanford-JPL hand were (1)

Fig. 3. Contact configurations.



that it be able to exert arbitrary forces or impress arbitrary small motions on the grasped object when the joints are allowed to move and (2) that it be able to constrain a grasped object totally by fixing (locking) all the joints. The first requirement means that the connectivity, C , between the grasped object and the palm must be 6 with the joints active. The second requirement dictates that with the finger joints locked the new connectivity, C' , must be ≤ 0 .

Many different hand-mechanism designs are possible, and in each one a rigid object may be grasped in many different ways. A given link of a finger may contact an object in any of the seven ways listed in Table 1. A finger with three links, for example can touch an object in 343 (7^3) unique ways. To determine the number of different grasps possible for a hand composed of k fingers, each of which can contact an object in n ways, we use the formula for the number of combinations, with repetitions, of n things taken k at a time:

$$\binom{n+k-1}{k} = \frac{(n)(n+1) \cdots (n+k-1)}{k!}$$

For a three-finger hand with three links on each finger, this number is 6,784,540. It is important to realize that this enumeration includes all one-, two-, or three-finger designs with one, two, or three links on each finger. Though all these mechanisms could be examined for acceptable designs, in designing the

Stanford-JPL hand it was felt that the large number of special cases revealed would not yield significant insight into the problem. It was decided to simplify the problem by assuming that all the contacts in a given design allow the same freedom of motion (one–five degrees of freedom). With three links per finger, each finger can touch the object in one of the eight configurations shown in Fig. 3. We may combine these configurations for several fingers to define many different grasping situations. For example, a two-finger design with two joints on each finger touching an object only on the last link would have a 2-2-0 configuration. With three fingers, the number of unique grasps (if we ignore contact type) is

$$\binom{8+3-1}{3} = 120.$$

For five different contact types (if we ignore zero- and six-degrees-of-freedom contacts), this yields 600 different designs to be investigated. The more complex hands with more links or fingers were not investigated because several acceptable designs were found within the above limitations.

Of the 600 designs considered, 39 were acceptable with $C = 6$ and $C' \leq 0$. Thirty-three of these were based on 5 degrees of freedom per contact with the grasped object, four were based on four degrees of freedom per contact with the object, and two on three degrees of freedom per contact. Designs based

on five degrees of freedom per contact were rejected because with frictionless contact points it would be impossible to exert moments on common objects such as cylinders and spheres. The four acceptable designs based on four degrees of freedom per contact are as follows.

Configuration	Number of Joints	C	C'
2-2-2	6	6	0
4-2-2	7	6	0
4-4-2	8	6	0
4-4-4	9	6	0

The two designs based on three degrees of freedom at each contact are as follows.

Configuration	Number of Joints	C	C'
4-4-0	6	6	0
4-4-4	9	6	-3

Of these, the 4-4-4 design was considered best for several reasons. It is the only design in which extra joints contribute to a more secure grasp ($C' = -3$). The negative connectivity implies a degree of excess constraint and allows control of internal forces necessary to keep frictional constraints active. It was also felt that maintaining the 3-degrees-of-freedom contact type (i.e., point contact with friction) would be easier than maintaining a four-degrees-of-freedom contact type (i.e., line on a plane without friction) and would lead to more robust grasping. In the final design, the last two axes were made parallel to each other and the second axis perpendicular to the first. This allowed the fingers to curl around objects for secure, or *power* grasping. The actual placement of fingers relative to one another was based on an optimization to be described later.

3. Accuracy Points and Singularities

In designing a manipulator, it is important to locate its workspace in the optimum location for the anticipated tasks. This becomes increasingly important when several manipulators or fingers must cooperate to manipulate a single object. Several measures of

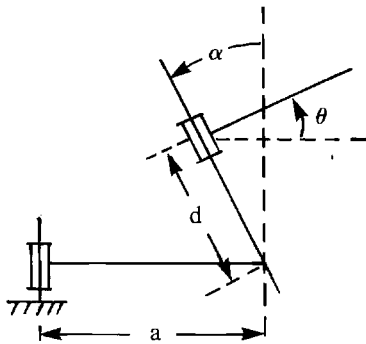
workspace are possible. The size of reachable volume is an important performance measure. If we ignore, for the moment, limits on joint range, we can see that a point on the end of a link that rotates about a revolute joint describes a circle. Two revolute joints in series allow a point on the end of the last link to touch all points on the surface of a general toroid. Adding a third revolute joint allows a point on the last link to reach all points in the volume resulting from revolving the toroid about the third axis (Roth 1975; Gupta and Roth, in press). It is this volume that must be judiciously placed relative to the working volume of the other fingers on the basis of anticipated grasped-object size.

To retain full mobility throughout its range of motion, the ideal finger would have no singularities in its workspace. Singularities occur where the rank of the Jacobian matrix becomes less than full (< 3 for the fingers of the Stanford-JPL hand). At these points, it would not be possible for the tip of the finger to move in an arbitrary direction for a small distance and thus limit motion of the grasped object. If motion is not possible in a particular direction, then it is impossible to exert a controlled force in that direction. Such singularities will always occur on the boundary of the workspace described above. A three-link finger with revolute joints will also always have a locus of singular points inside the workspace (Shimano 1978). For the finger design selected, this locus is the line passing through the first axis of revolution (see Fig. 7). In selecting the placement of fingers relative to one another, we try to keep this interior locus of singularities away from the anticipated grasping points on objects so that it will be possible to make arbitrary small motions of the grasped object.

3.1. ERROR PROPAGATION

Another measure of workspace quality is the accuracy with which forces can be exerted. It has been found that at certain interior points in the workspace forces may be exerted with maximum accuracy (details forthcoming in a Ph.D. thesis by J. K. Salisbury, now in preparation). By looking at the condition number of the force transformation, J^T , it is

Fig. 4. Linkage dimensions.



possible to compare error propagation with different manipulator configurations. One of the anticipated uses of this hand is in force-controlled tasks, and the location of most accurate operation points is a useful design consideration.

The transpose of the Jacobian matrix, J^T , is a linear transform from joint torques, $\underline{\tau}$, to forces, \underline{F} , exerted at the fingertip. If we consider error propagation in linear systems (Strang 1976), we note that the relative error is bounded by the product of the condition number of the Jacobian transpose matrix and the relative error in joint torque.

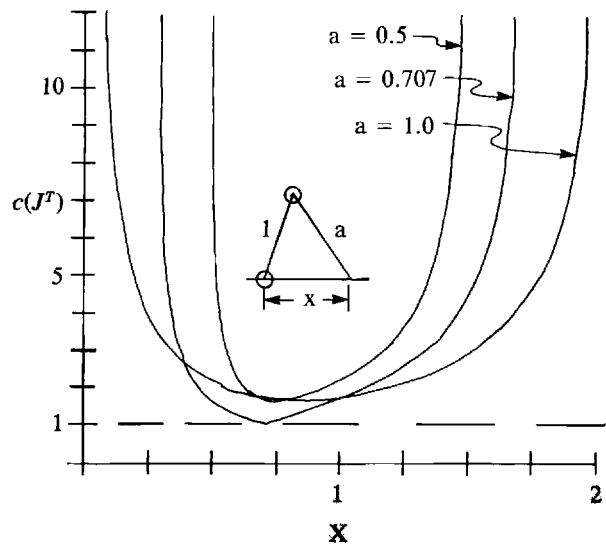
$$\frac{\|\delta \underline{F}\|}{\|\underline{F}\|} \leq c(J^T) \frac{\|\delta \underline{\tau}\|}{\|\underline{\tau}\|} \quad (3)$$

where

- $\delta \underline{F}$ = fingertip-force error vector;
- \underline{F} = fingertip-force vector;
- $\delta \underline{\tau}$ = joint-torque error vector;
- $\underline{\tau}$ = joint-torque vector;
- $c(J^T)$ = condition number ($= \|J^T\| \|J^{-T}\|$);
- $\|\cdot\|$ = norm.

Points in the workspace that minimize the condition number of the Jacobian matrix are the best conditioned to minimize error propagation from input torques to output forces. The best conditioning possible occurs when $c(\cdot) = 1$. In general, this occurs at points in the workspace where the Jacobian matrix satisfies two conditions: (1) its columns are orthogonal and (2) its column vectors are of equal magni-

Fig. 5. Condition numbers for mechanisms with two parallel revolute joints ($\alpha = 0^\circ$).



tude. Such best-conditioned points, which we will call *isotropic points*, may or may not exist for a given design. For example, three mutually perpendicular prismatic joints in series would have a condition number of 1 everywhere within the range of motion. A general two-link mechanism with revolute joints that have the dimensions shown in Fig. 4 will satisfy the orthogonality conditions at points within its workspace (real θ) if

$$a^2 \leq d^2 \tan^2(\alpha) + 1. \quad (4)$$

Within the constraints of (Eq. 4), mechanisms that satisfy the orthogonality and magnitude conditions simultaneously for some value of θ will have an isotropic point. Figure 5 shows the condition number for points in the workspace of several two-revolute-joint mechanisms with axes parallel. It can be seen that the mechanism with $a = 0.707$ has a true isotropic point within its workspace. A two-link mechanism with perpendicular axes always satisfies the orthogonality constraint and allows us to place the isotropic point anywhere on the parabola shown in Fig. 6 by appropriately selecting the last link length, a .

The fingers selected for the Stanford-JPL hand combine the mechanisms shown in Figs. 5 and 6.

Fig. 6. Mechanism with two perpendicular revolute joints ($\alpha = 90^\circ$).

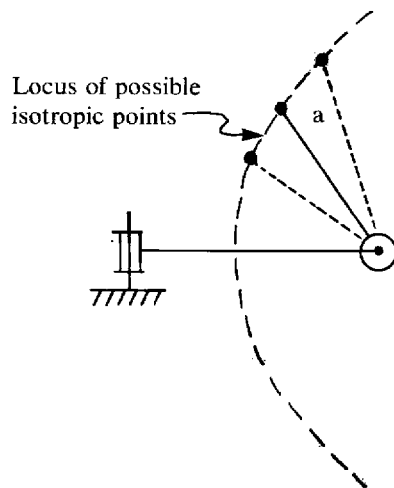
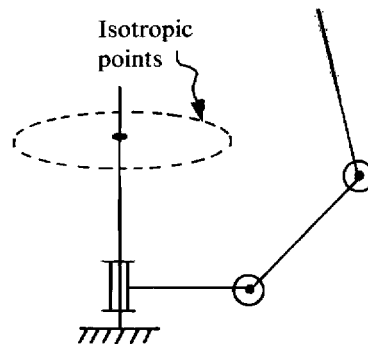


Fig. 7. Three-joint finger mechanism.



The mechanism and the resulting circular locus of isotropic points is shown in Fig. 7. By positioning the three fingers relative to one another appropriately, the three isotropic loci may be made simultaneously to touch an object to be manipulated. A nominal object (1-in sphere) was selected as a guide in positioning these loci.

We can find the best-conditioned point in the workspace of an existing manipulator design numerically. Even if strict isotropic points do not exist, one or more minima for $c(J^T)$ will exist. This may also serve as a basis for optimizing partially constrained motion. For example, if we are exerting forces on an object with symmetry about an axis (i.e., a cylinder) we may rotate it about that axis to minimize the condition number, thus improving the force-application accuracy. Ultimately, the minimization of condition numbers in the manipulator's workspace could serve as an optimization criterion in link design.

3.2. NOISE PROPAGATION

Isotropic points are also points that minimize the dispersion of noise through the system. If we assume the existence of independent, identically distributed noise sources with 0 mean at each of the joint actuators (resulting from quantization error, limit

cycles, random friction sources, and so on), we can describe the transformation of the covariance matrix, Λ_T , from joint space to fingertip-force space, Λ_F , as

$$\Lambda_F = J\Lambda_T J^T. \quad (5)$$

The resulting multidimensional probability density function will be spherically symmetric if the eigenvalues of JJ^T are equal (the eigenvalues of JJ^T are equivalent to those of $J^T J$). Thus, the isotropic points are also points at which the likelihood of error of a given magnitude is the same in all directions.

Finally, isotropic points can be viewed as points where, given a fixed sum of power dissipations at the actuators, we may exert forces of equal magnitude in all directions. This relationship results from modeling actuator power dissipation at stall as being proportional to the torque squared (i.e., torque is proportional to current and power is proportional to current squared). If we combine power = $\underline{\tau}^T \underline{\tau}$ = constant and $\underline{\tau} = J^T \underline{F}$, we get the quadratic form

$$\underline{F}^T J J^T \underline{F} \leq \text{constant}. \quad (6)$$

Again, if the eigenvalues of JJ^T are all equal (isotropic points) the maximum values of $\|\underline{F}\|$ will be the same in all directions.

It is assumed in the above discussion that the actuators act in joint space as do the associated noise sources. In the design selected, the actuators do not act directly in joint space but rather through a transmission system described by the matrix R^{-1} (see

Section 5), which must multiply J^T . With cable tension vector, $\underline{T} = R^{-1}J^T\underline{E}$, isotropic points will actually occur where all the eigenvalues of $JR^{-T}R^{-1}J^T$ are equal.

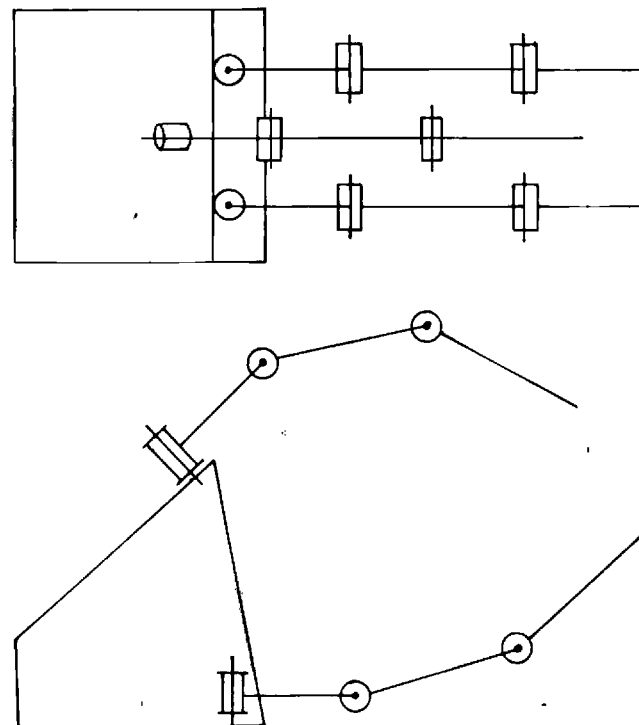
4. Optimization of Hand Kinematics

With a kinematic structure, the problem of dimensional synthesis can be approached in several ways. In the case of spatial linkages, joint-range limits and link collisions make an analytical approach difficult. An interesting approach is to model the kinematics in software and apply parameter optimization techniques in order to choose parameter values. OPHAND is a program in which such techniques are used to choose parameter values based on maximizing a performance criterion.

An object in the hand may be controlled in 6 degrees of freedom only when held in tip prehension with grasp contact points on the last link of each finger. Because this is an important class of grasps, the performance criterion adopted in the OPHAND program considers only fingertip grasps. Potential designs are scored on the basis of *working volume*, defined as the volume within which the object may be positioned given a fixed grasp. Although this is possibly the most important criterion, it clearly does not encompass all the factors that should be considered when choosing hand designs. For example, besides *manipulative grasps*, which allow 6-degrees-of-freedom control of the object, *power grasps*, in which the object is constrained by several links and/or the palm, are important too. Thus, OPHAND results are used to supplement the design procedure rather than to guide it.

OPHAND makes use of models of the finger locations, kinematics, joint limits, object size, and desired grip points. A large number of discrete positions and orientations are tested to determine the volume within which fingertip grasps are possible for a given hand design. Various parameters of the hand are adjusted by a conjugate gradient algorithm (Powell 1964), which chooses search directions in parameter space along which one-dimensional searches are performed. This algorithm is quadratically convergent but, unlike steepest descent

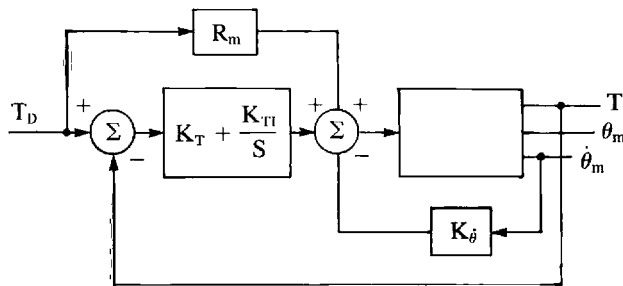
Fig. 8. Top and side views of the Stanford-JPL hand showing the thumb placement determined by OPHAND.



methods, does not require that gradient information be available at the search points.

The dimensionality of the Stanford-JPL hand's parameter space is 36. These parameters specify finger locations relative to one another, link lengths, and joint limits. Many of these parameters are selected with regard to mechanical design considerations or other criteria. OPHAND has been applied to investigating hand performance in restricted subspaces of one to five parameters. For example, if we fix the location of the two finger bases on the palm (Fig. 8), we can use OPHAND to find a thumb location. By carefully choosing which parameters OPHAND is to select, we can ensure that the resulting hand design meets some of the heuristic criteria that are not reflected in the chosen performance index. The position and the orientation of the thumb base found by OPHAND more than doubled the performance index of an original heuristic design while retaining features thought to be favorable (palm area,

Fig. 9. Tendon-control system.



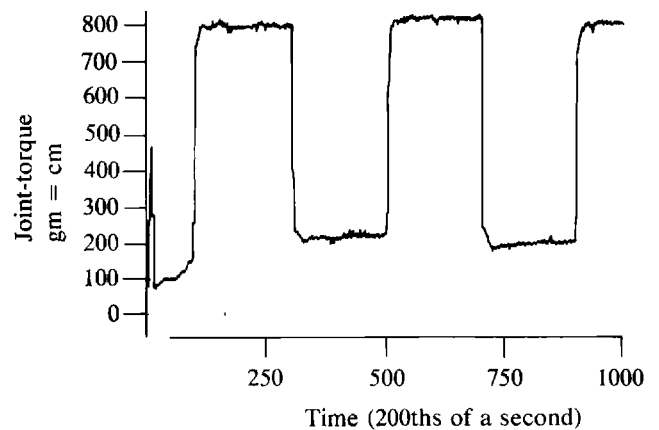
reasonable finger placement for power grasps, and so on).

Another useful design tool is a simulator with graphic output developed at Stanford by Soroka (1980). This system displays potential hand designs and allows the user to manipulate joints interactively and view the hand from arbitrary camera locations.

5. Hand Control

In active-force-control schemes for manipulators, sensing is done either at the wrist (Whitney 1976; Craig and Raibert 1979; Salisbury 1980; Raibert and Craig 1981) or at the joints (Paul and Wu 1980). In wrist-based methods, the sensors are placed close to the point of interest so that force sensing is easier and more accurate, but stability problems occur due to modeling errors or simplifications, resulting in low-gain servos. Joint-based systems, in which one sensor is associated with one actuator, tend to result in high-gain, high-bandwidth servos. Use of such servos may be viewed as an attempt to make up for less-than-perfect actuator and transmission systems by use of sensing and control to remove the effects of gearing friction, backlash, and actuator nonlinearity. Joint-based systems, however, require that the effects of gravity (and possibly dynamic forces) be modeled in order to extract force information at the hand from sensor data. The tendon-based actuation scheme proposed here for the Stanford-JPL hand has force sensors that are used in a servo loop that encloses the major source of friction (motor gearing and tendon conduit). The force sensors are also close to the point of interest. Thus, both control and sensing benefit.

Fig. 10. Response of prototype joint to steps in output torque. Units of torque are gm-cm. Time axis is in samples taken at 200 Hz.



The hand-control system in the Stanford-JPL hand is based on tendon-level control. Each tendon is controlled with a feed-forward term and a linear regulator with constant gains. The structure of the tendon controller (Fig. 9) includes an integral term to remove steady-state errors due to friction. Additional feed-forward terms may be added to compensate for dynamic forces or nonlinear effects such as coulomb friction.

A prototype tendon-actuated joint has been built and tested at Stanford. It makes use of active tension sensing and the control architecture described above. Figure 10 shows the response of this joint to step changes in desired torque output at the joint while it is acting on a stiff (aluminum-on-steel) environment.

The tension in the tendons determines the torques at the joints and the forces on the bearings at each joint. Determination of four tendon tensions, given three desired joint torques, is an underspecified problem. To obtain a unique solution, we specify one of the bearing forces, whose value is computed to ensure that all tendon tensions are positive. We then write the relationships:

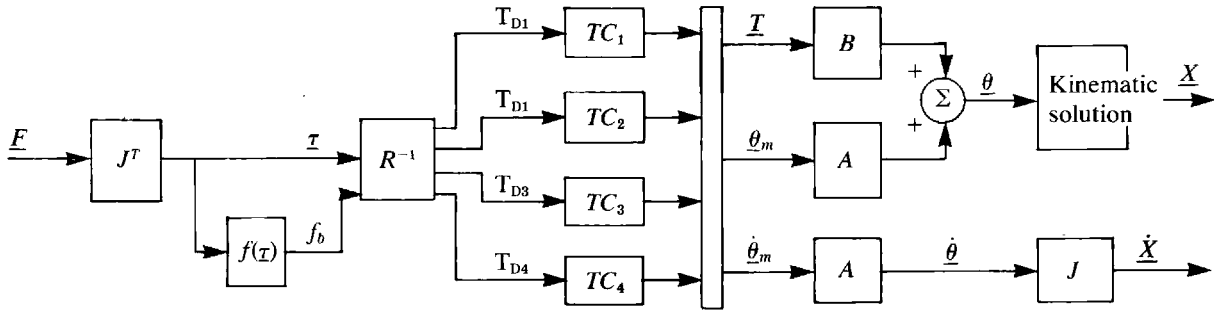
$$[\underline{\tau} \ f_b]^T = R\underline{T} \quad (7)$$

$$\underline{T} = R^{-1}[\underline{\tau} \ f_b]^T \quad (8)$$

where

$\underline{\tau}$ = vector of joint torques (3×1);

Fig. 11. Four tendon controllers used to form a finger system.



f_b = scalar force on bearing of joint 1;
 R = constant matrix, determined from cabling and pulley radii (4×4);
 \underline{T} = vector of tendon tensions (4×1).

Using (Eq. 8), we can write the expression for the tension in the i th tendon in the form:

$$T_i = G_i(\underline{x}) + k_i f_b. \quad (9)$$

The constants that make up the linear functions G and the constants k are the elements in R^{-1} . We determine an expression for f_b by requiring that each T_i be positive:

$$f_b = \max_i \frac{-G_i(\underline{x})}{k_i}. \quad (10)$$

The value of f_b will always be positive and will ensure that all tendons are in positive tension.

In order to estimate joint position and velocity from information sensed in tendon space, we define the constant matrices A and B :

$$\underline{\theta} = A \underline{\theta}_m + B \underline{T} \quad (11)$$

$$\dot{\underline{\theta}} = A \dot{\underline{\theta}}_m \quad (12)$$

where

$\underline{\theta}$ = vector of joint angles;
 $\dot{\underline{\theta}}$ = vector of joint angular velocities;
 $\underline{\theta}_m$ = vector of motor angles;
 $\dot{\underline{\theta}}_m$ = vector of motor angular velocities.

Matrices A and B are determined by cabling struc-

ture and various pulley radii and make use of redundant information by averaging. The B matrix allows the inclusion of tendon stretch in the joint position estimation. Figure 11 shows four tendon controllers used to form a finger system. This finger system includes transformations so that it accepts desired forces in Cartesian space and outputs Cartesian position and velocity. Below are the R , R^{-1} , A and B matrices for one finger of the Stanford-JPL hand. Note that all matrices are constant for a given finger design, and so are not calculated on line.

$$R = \begin{bmatrix} -R_1 & R_2 & R_2 & -R_1 \\ R_1 & R_2 & -R_2 & -R_1 \\ 0 & R_2 & -R_2 & 0 \\ 1 & 1 & 1 & 1 \end{bmatrix} \quad (13)$$

$$R^{-1} = \begin{bmatrix} \frac{-1}{2R_2 + 2R_1} & \frac{1}{2R_1} & \frac{-1}{2R_1} & \frac{R_2}{2R_2 + 2R_1} \\ \frac{1}{2R_2 + 2R_1} & 0 & \frac{1}{2R_2} & \frac{R_1}{2R_2 + 2R_1} \\ \frac{1}{2R_2 + 2R_1} & 0 & \frac{-1}{2R_2} & \frac{R_1}{2R_2 + 2R_1} \\ \frac{-1}{2R_2 + 2R_1} & \frac{-1}{2R_1} & \frac{1}{2R_1} & \frac{R_2}{2R_2 + 2R_1} \end{bmatrix} \quad (14)$$

$$A = \begin{bmatrix} \frac{-R_m}{4R_1} & \frac{R_m}{4R_2} & \frac{R_m}{4R_2} & \frac{-R_m}{4R_1} \\ \frac{R_m}{4R_1} & \frac{R_m}{4R_2} & \frac{-R_m}{4R_2} & \frac{-R_m}{4R_1} \\ 0 & \frac{R_m}{2R_2} & \frac{-R_m}{2R_2} & 0 \end{bmatrix} \quad (15)$$

$$B = \begin{bmatrix} \frac{1}{4kR_1} & \frac{-1}{4kR_2} & \frac{-1}{4kR_2} & \frac{1}{4kR_1} \\ \frac{-1}{4kR_1} & \frac{-1}{4kR_2} & \frac{1}{4kR_2} & \frac{1}{4kR_1} \\ 0 & \frac{-1}{2kR_2} & \frac{1}{2kR_2} & 0 \end{bmatrix} \quad (16)$$

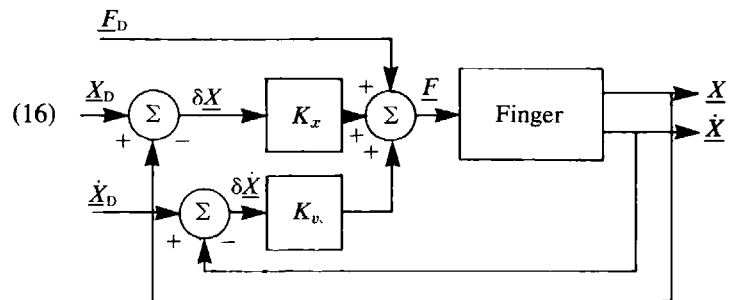
where:

- R_1, R_2 = radius of pulleys at joints;
- R_m = equivalent radius of motor pulley (includes gearing at motor);
- k = stiffness of tendons.

There is a simple control structure for a single finger that is commanded in Cartesian coordinates but does not require the computation of an inverse kinematic solution or an inverse Jacobian matrix. The method also combines the best features of previous work on active force control systems for manipulators, the hybrid position/force approach (Craig and Raibert 1979; Raibert and Craig 1981) and the stiffness approach (Salisbury 1980). Figure 12 is a block diagram of such a system. Although force control appears to be open-loop at this level, there are closed force-control loops within the finger subsystem. The matrix K_x is diagonal and sets the stiffness of the fingertip in Cartesian space. K_v is calculated as a linear function of K_x in order to keep the response of the position servo approximately critically damped even as the commanded stiffness, K_x , changes. If K_x is set to 0, the finger may be operated in pure force servo mode via commands at the F_d input. By selectively zeroing elements of K_x and F_d , orthogonal Cartesian directions may be controlled in different modes.

Hand control is the problem of simultaneous control of several fingers, each with several degrees of freedom. The problem is analogous to the problem of controlling two or more manipulators cooperatively (Ishida 1977). We are concerned here with the control of three fingers with three degrees of freedom. These nine degrees of freedom allow the specification of the six-degrees-of-freedom behavior of the grasped object relative to the palm as well as the specification of three forces within the object acting along the edges of the grasp triangle.

Fig. 12. Cartesian finger-control system. All data paths represent (3×1) vectors.



Control of individual fingers, as suggested in Fig. 12, is useful when the fingers are not coupled, for example, for following position trajectories through space or striking a piano key with one finger. When objects are grasped, the fingers are coupled and should be controlled differently. Control of coupled motions with uncoupled controllers is possible with some fingers in position mode and others in force-control mode, but such schemes seem to lack generality.

So that all fingers can act cooperatively, we must expand the method proposed for single-finger control in Fig. 12 to allow coupled control of the fingers. We wish to control parameters of position, stiffness, or force of the object in a Cartesian coordinate system. Additionally, we must specify three parameters of the grasp, for example a stiffness behavior between fingers that maintains a grasp force on the object. If fixed grasp points are assumed, this coupling between fingers may be expressed as a 9×9 grasp matrix, G^{-T} (inverse of G^T) (Eq. 18), which relates fingertip forces to external forces on the object and internal grasp forces (Eq. 17). The matrix is specified by the relationship between object grasp points and desired center of compliance, and so is computed once for a given grasp.

We may now expand the finger controller shown in Fig. 12 to form a hand controller. This requires that we invert the grasp matrix (once per given grasp), which is always possible if the three grasp points are not chosen to be colinear. Then, from (Eq. 17), we obtain:

$$F = G^T \mathcal{F}. \quad (18)$$

$$\underline{\mathcal{F}} = G^{-T} \underline{F} \quad (17)$$

$$G^{-T} = \begin{bmatrix} 1 & 0 & 0 & 1 & 0 & 0 & 1 & 0 & 0 \\ 0 & 1 & 0 & 0 & 1 & 0 & 0 & 1 & 0 \\ 0 & 0 & 1 & 0 & 0 & 1 & 0 & 0 & 1 \\ 0 & -r_{1z} & r_{1y} & 0 & -r_{2z} & r_{2y} & 0 & -r_{3z} & r_{3y} \\ r_{1z} & 0 & -r_{1x} & r_{2z} & 0 & -r_{2x} & r_{3z} & 0 & -r_{3x} \\ -r_{1y} & r_{1x} & 0 & -r_{2y} & r_{2x} & 0 & -r_{3y} & r_{3x} & 0 \\ r_{12x} & r_{12y} & r_{12z} & -r_{12x} & -r_{12y} & -r_{12z} & 0 & 0 & 0 \\ r_{13x} & r_{13y} & r_{13z} & 0 & 0 & 0 & -r_{13x} & -r_{13y} & -r_{13z} \\ 0 & 0 & 0 & r_{23x} & r_{23y} & r_{23z} & -r_{23x} & -r_{23y} & -r_{23z} \end{bmatrix}$$

where

\underline{r}_i = vectors from compliance center to i th grasp point;

\underline{r}_{ij} = unit vectors pointing from i th to j th grasp point;

\underline{F}_i = force vectors applied at i th fingertip;

\underline{f} = force vector acting on object at compliance center;

\underline{t} = torque vector on object at compliance center;

f_{ij} = scalar force of grasp between finger i and j ;

G^{-T} = grasp matrix;

and

$$\underline{\mathcal{F}} = [\underline{f} \quad \underline{t} \quad f_{12} \quad f_{13} \quad f_{23}]^T;$$

$$\underline{F} = [\underline{F}_1 \quad \underline{F}_2 \quad \underline{F}_3]^T;$$

$$\underline{f}_{ij} = (\underline{F}_i - \underline{F}_j) \cdot \underline{r}_{ij}.$$

The grasp matrix can be viewed as a Jacobian matrix relating fingertip forces to object forces (including internal forces). We can describe the desired generalized stiffness behavior of the object as

$$\underline{\mathcal{F}} = K_x \delta \underline{\mathcal{X}}. \quad (19)$$

For small displacements and virtual work considerations,

$$\underline{\delta x} = G \delta \underline{\mathcal{X}} \quad (20)$$

where

K_x = (9×9) diagonal stiffness matrix;

$\delta \underline{\mathcal{X}}$ = vector of small displacements of the object and grip points;

$\underline{\delta x}$ = vector of small displacements of the fingertips.

Combining (Eqs. 18–20) yields the relationship needed for control:

$$\underline{F} = G^T K_x G \underline{\delta x}. \quad (21)$$

Fig. 13. Cartesian hand controller. All data paths represent (9×1) vectors.

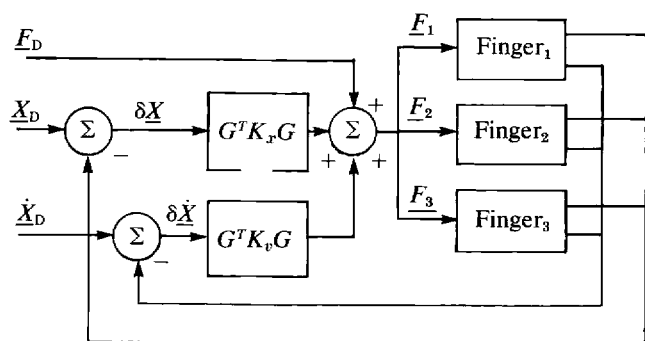


Figure 13 shows the hand controller based on (Eq. 21). It does not require any inverse kinematic or inverse Jacobian solutions. The inputs are desired position of the fingertips, which can be computed based on desired object position by straightforward Cartesian frame operations. A fingertip force input is also shown, as in the finger controller.

6. Conclusions

Several considerations related to the design of articulated hands have been introduced here: mobility, force-application accuracy, singularities, noise propagation, parameter optimization, and control-system structure. The Stanford-JPL hand has been designed with these considerations in mind. It makes use of those results that are practical when balanced against realistic design limitations. The control architecture described should allow active position and force control of a grasped object for the fine motions of automated assembly. The actual implementation of these ideas is in progress and will be evaluated in future reports.

REFERENCES

- Childress, D. S. 1972 (Oct.). Artificial Hand mechanisms. Paper delivered at Mechanisms Conf. and Int. Symp. on Gearing and Transmissions, San Francisco, Calif.
- Craig, J. J., and Raibert, M. H. 1979 (Nov.). A systematic method for hybrid position/force control of a manipulator. Paper delivered at IEEE COMPSAC Conf., Chicago, Ill.
- Crossley, F. R. E., and Umholtz, F. G. 1977. Design for a three fingered hand. *Mechanism and Machine Theory* 12:85-93.
- Drake, S. 1977. Using compliance in lieu of sensory feedback for automatic assembly. Laboratory Report T-657. Cambridge, Mass.: Charles Stark Draper Laboratory.
- Gupta, K. C., and Roth, B. In press. Design considerations for manipulator workspace. *Trans. ASME, J. Mechanical Design*.
- Hunt, K. H. 1978. *Kinematic geometry of mechanisms*. Oxford: Oxford University Press.
- Ishida, T. 1977. Force control in coordination of two arms. *Proceedings 5th Int. Joint Conf. on Artificial Intell.* MIT, pp. 717-722.
- Lakshminarayana, K. 1978 (Sept.). Mechanics of form closure. Paper delivered at ASME Design Engineering Technical Conf. Minneapolis, Minn.
- Morecki, A. 1980. Synthesis and control of the anthropomorphic two-handed manipulator. *Proc. 10th Int. Symp. on Industrial Robots*.
- Okada, T. 1979. Computer control of multi-jointed finger system. Paper delivered at Sixth Int. Joint Conf. on Artificial Intell., Tokyo, Japan.
- Paul, R. L., and Wu, C. H. 1980 (Nov.). Manipulator compliance based on joint torque contr. Paper delivered at IEEE Conf. on Decision and Control, Albuquerque, N.Mex.
- Powell, M. J. D. 1964. An efficient method for finding the minimum of a function of several variables without calculating derivatives. *Compu. J.* 7:152-162.
- Raibert, M. H., and Craig, J. J. 1981. Hybrid position/force control of manipulators. *Trans. ASME* 102:126-133.
- Reuleaux, F. 1963. *The kinematics of machinery*. New York: Dover.
- Roth, B. 1975. Performance evaluation of manipulators from a kinematic viewpoint. *Performance Evaluation of Programmable Robots and Manipulators*. Bethesda, Md.: National Bureau of Standards, pp. 39-61.
- Rovetta, A. 1977. On specific problems of design of multi-purpose mechanical hands in industrial robots. *Proc. 7th Int. Symp. Industrial Robots*.
- Salisbury, J. K. 1980 (Nov.). Active stiffness control of a manipulator in Cartesian coordinates. Paper delivered at IEEE Conference on Decision and Control, Albuquerque, N.Mex.
- Salisbury, J. K., and Ruoff, C. 1981. The design and con-

-
- trol of a dextrous mechanical hand. *Proc. 1981 ASME Comput. Conf.*
- Schlesinger, G. 1919. Der Mechanische Aufbau der Kunstlichen Glieder. *Ersatzglieder und Arbeitshilfen*, part II. Berlin: Springer.
- Shimano, B. 1978. The kinematic design and force control of computer controlled manipulators. Memo 313. Stanford, Calif.: Stanford University Artificial Intelligence Laboratory.
- Skinner, F. 1975. Designing a multiple prehension manipulator. *Mechanical Engineering*, Sept.
- Soroka, B. I. 1980 (Nov. 17–20). Debugging manipulator programs with a simulator. Paper delivered at Autofact West Conf. Soc. of Manufacturing Engineers, Anaheim, Calif.
- Strang, G. 1976. *Linear algebra and its applications*. New York: Academic.
- Whitney, D. E. 1976. Force feedback control of manipulator fine motion. *Trans. ASME, J. Dyn. Syst., Meas., Control* 99(2):91–97.